Giant magnetoresistance and Co-cluster structure in phase-separated Co-Cu granular alloys

T. A. Rabedeau, M. F. Toney, R. F. Marks, S. S. P. Parkin, R. F. C. Farrow, and G. R. Harp
IBM Research Division, Almaden Research Center, San Jose, California 95120-6099
(Received 17 June 1993)

We examine the effect of Co-cluster morphology on giant magnetoresistance (MR) in phase-separated Co-Cu films. The Co clusters were characterized through grazing incidence, anomalous, small-angle x-ray scattering. With thermal annealing the Co cluster diameter increases from 21 to ~250 Å with a concomitant drop from ~35% to 1% in the 4.2 K MR. The MR scales approximately as the inverse cluster size. Comparison with theory indicates that interfacial spin-dependent electron scattering is the dominant scattering mechanism underlying giant MR for cluster diameters up to at least 250 Å.

The observation of giant magnetoresistance (MR) and oscillatory interlayer magnetic coupling in Fe/Cr multilayers[1,2] has stimulated considerable work on the properties of this and related magnetic multilayers. The interest in magnetic thin films was heightened by the recent discovery of giant MR in simple binary alloy films that are composed of magnetic clusters embedded in a nonmagnetic metal matrix.[3,4] The resistance of these films depends upon the distribution of the magnetic moments of the individual clusters. The resistance is minimized for parallel alignment of the cluster magnetic moments, exactly analogous to giant MR in multilayers. Just as for multilayers, the MR depends critically on the film structure; however, there has been little structural characterization of alloy films exhibiting giant MR. In particular, determination of the size of the magnetic clusters and the dependence of the MR on this size is essential to understanding the origin of giant MR in alloy films.[3,5] In this paper we describe the first application of grazing incidence, anomalous, small-angle x-ray scattering (SAXS) in a cluster characterization of Co-Cu granular alloy films. This permits the investigation of the effect of cluster size on giant MR in granular alloys and, through comparison with phenomenological theory, identification of the important sources of spin-dependent electron scattering that cause the giant MR of these materials.

The choice of Co-Cu alloys for this study was primarily motivated by the tunability of the x-ray scattering contrast of Co-Cu, which is well suited to grazing incidence SAXS measurements. The samples consisted of five 800 Å films of $Co_{16}Cu_{84}(111)$ grown simultaneously at 200 °C by coevaporation from separate Co and Cu sources of a molecular beam epitaxy (MBE) system at ~0.02 and ~0.10 Å/s, respectively. The alloy films were grown on 30 Å Pt(111) seed layers on sapphire (0001) substrates and were capped with 20 Å of pure Cu. Sputter-deposited films usually require post-growth thermal anneals to phase separate the magnetic and nonmagnetic components and obtain appreciable MR.[3] In contrast, the films grown for this study exhibited substantial MR without annealing, which results from spontaneous phase separation of the immiscible Co and Cu during growth.[6] Postgrowth thermal annealing was employed to alter the film morphology in order to explore the relationship of MR to cluster size. Specifically, four of the samples were annealed in ultrahigh vacuum (UHV) for 10 min at maximum temperatures of 250, 350, 450, or 550 °C. To minimize oxidation, the samples were maintained in UHV or in inert gas except for brief air exposures during handling.

The MR of the films was measured using a four in-line contact geometry with the saturation MR, $\Delta R/R_s$, defined as the maximum change in resistance for current and field in the plane of the film divided by the high-field resistance. Both the MR and the saturation field decrease monotonically with increasing anneal temperature. In contrast with cosputtered films,[3] the high-field resistivity of the films displays only a weak anneal dependence. In particular, the high-field resistivity at 4.2 K is 5.5–6.8 $\mu\Omega$ cm except for the film annealed at 550 °C, for which Pt buffer-layer dissolution[7] increased the resistivity to 13.4 $\mu\Omega$ cm. Thus, for our MBE films, the MR dependence on thermal annealing stems primarily from changes in ΔR rather than from variations of both ΔR and R_s as is typical of cosputtered films.

The crystallographic order of the films was investigated by x-ray diffraction.[7] The films grew epitaxially on the Pt buffer with $\lesssim 0.5°$ surface-normal and in-plane mosaic spreads. Consistent with the resistivity results, the post-growth anneal had little affect on the crystal coherence lengths [e.g., the inverse half-widths of the (111) peak ranged from 150 to 200 Å]. With the exception of the 550 °C film, the diffraction data indicate the Co and Cu lattices are coherent.

The coherency of the Co and Cu lattices precludes the use of diffraction to investigate chemical cluster size in all but the 550 °C film. Similarly, electron microscopy proved ineffective, owing to the weak Co-Cu contrast while fluorescence-microprobe analysis is insensitive to small clusters. On the other hand, SAXS is a technique which is sensitive to clusters as small as 10 Å. To apply this technique, we enhanced the otherwise weak Co-Cu scattering contrast by utilizing the large changes in the Co scattering factor for photon energies near the Co adsorption edge.[8] The SAXS intensity is proportional to the Fourier transform of the autocorrelation of the deviation of the local scattering strength from the average scattering strength, $f(r)n(r)-\overline{fn}$, where $n(r)$ and $f(r)$ are the local atomic number density and atomic form factors, respectively.[8,9] Measurements using a conventional

0163-1829/93/48(22)/16810(4)/$06.00

transmission SAXS geometry proved impossible for the alloy films due to the small scattering volume of the MBE films coupled with the x-ray attenuation of the sapphire substrates required for epitaxy. Rather, a grazing incidence reflection geometry[10] was employed as depicted in Fig. 1. Grazing incidence SAXS involves intensity measurements near the specularly reflected beam where surface diffuse scattering is an intense source of background (see Fig. 2) (Ref. 11). This background, which originates from roughness at the film-vapor interface, was characterized in companion scattering measurements with the photon energy tuned to minimize the Co-Cu scattering contrast and, hence, the cluster scattering.[12]

The SAXS measurements reported here were conducted at the National Synchrotron Light Source on beam line X20A. Typical resolutions of 2.2 mrad along the film normal and 0.4 mrad in the film plane were obtained through use of slits and a Ge(111) analyzer crystal. After convolution over the instrumental resolution, the x-ray penetration depth into the film was ~ 200 Å ($1/e$ depth) while the refraction corrected minimum total momentum transfer was ~ 0.045 Å^{-1}. Measurements were performed using 7692 and 8710 eV photons. The effective Co-Cu scattering contrast at these two energies is calculated to be $40.2r_0^2$ (7692 eV) and $0.0r_0^2$ (8710 eV), where r_0 is the Thomson radius.[13]

Typical SAXS data collected at each energy are shown in Fig. 2. After application of a scale factor common to all background data sets,[14] a smooth curve fit to the background for each film was subtracted from the 7692 eV data. The 450°C data of Fig. 2 are replotted in Fig. 3 after background subtraction and conversion to $q=\sqrt{(q_{\text{in plane}}^2+q_z^2)}$ where q_z is the refraction-corrected momentum transfer perpendicular to the film and $q_{\text{in plane}}$ is the in-plane momentum transfer. While reverse transformation of $I(q)$ yields the autocorrelation function $\gamma(r)$, extraction of a characteristic Co-cluster radius from $\gamma(r)$ is complicated by cluster shape and size distribution and intercluster interference.[9] Instead, we employ the well-established relation between the integrated intensity, Porod's law for the asymptotic slope of $I(q)$, and the cluster size.[9] Explicitly, the Porod radius (R_p) of the Co clusters is

$$\frac{\langle r^3\rangle}{\langle r^2\rangle}=\frac{3\int dq\, q^2 I(q)}{\pi(1-\phi)}\left[\lim_{q\,\text{large}} q^4 I(q)\exp(\sigma^2 q^2)\right]^{-1},$$

where ϕ is the volume fraction of Co, and σ is the root-mean-square (rms) interface width of the Co clusters (see below); the limit is evaluated at large enough q that only intracluster interference contributes to $I(q)$, the brackets denote averaging over the scattering volume, and we assumed spherically shaped clusters with error function electron-density profiles at the Co-Cu interfaces.[9,15] The Porod analysis yields the ratio of the cluster volume to interfacial area. Calculation of a Porod radius entails the assumption of spherical clusters and the inclusion of a geometrical factor 3 in the equation above. This assumption is a simplification of the actual cluster morphology. We note, however, that analysis of the Co shoulder of the 550 °C sample diffraction data yields a Co cluster radius

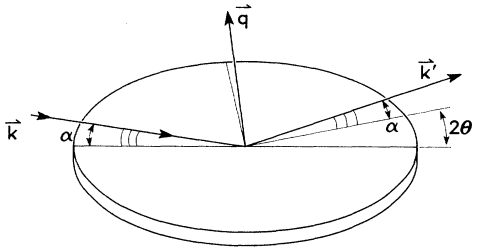

FIG. 1. A schematic of the SAXS geometry. **k**, **k'**, and **q** are the incident, outgoing, and momentum-transfer wave vectors, respectively. The incident and exit angles α are typically 0.03° greater than the critical angle for x-ray total external reflection. The specular reflection is obtained for $2\theta=0$.

of ~ 100 Å, in good agreement with the 124 ± 17 Å Porod radius. This suggests that the assumption of spherical clusters provides a reasonable approximation to the actual cluster morphology.

The inset of Fig. 4 shows the evolution of the Porod radii calculated from the SAXS data as a function of anneal temperature. These data indicate that the size of the Co clusters increases monotonically with thermal annealing. It is also apparent from Fig. 4 that the decrease in MR with annealing correlates with increased Co-cluster size.

Before discussing the relationship of MR to cluster size, we note that the MR is affected by the structure of the Co-Cu interfaces[5,16] and that SAXS data provide insight into this structure. The Co-Cu interface rms width was extracted using Porod's law: $q^4 I(q)=K\exp(-\sigma^2 q^2)$ with K a constant and q large.[9] The asymptotic slope of $q^4 I(q)$ yields the interface width with zero (negative) slope, indicating an abrupt (diffuse) interface. $q^4 I(q)$ vs q

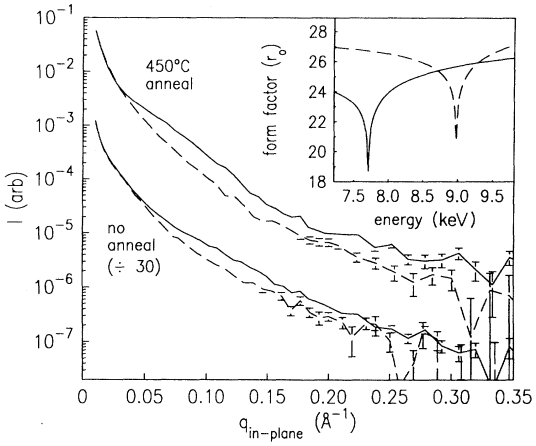

FIG. 2. The scattered intensity for the unannealed and 450 °C annealed films. The solid (broken) line represents the scattering with the Co-Cu contrast maximized (minimized). The minimal contrast data have been scaled by 3.275 relative to the maximal contrast data. With increasing anneal, the scattered intensity originating from clustering shifts to smaller $q_{\text{in plane}}$. The inset depicts the real part of the calculated Co (——) and Cu (— — —) atomic form factors after convolution with the 7.3 eV rms instrumental energy resolution.

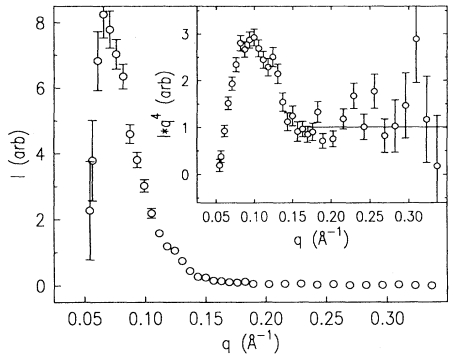

FIG. 3. Background-subtracted scattering data for the 450 °C film. The inset depicts these data multiplied by q^4. The line represents the best fit for $K\exp(-\sigma^2q^2)$ yielding $\sigma=0$ (i.e., atomically abrupt interfaces).

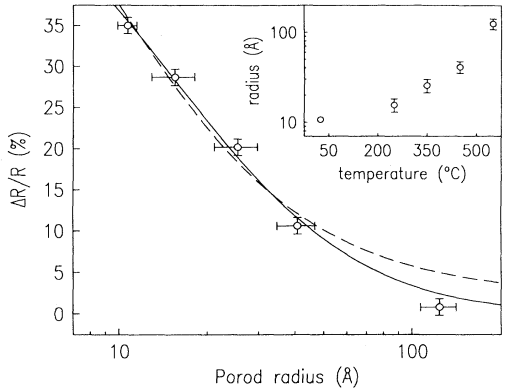

FIG. 4. The saturation MR vs the measured Porod radii (○). The saturation MR data were measured using a 1.6 T maximum field. The solid line depicts the results of the fit with only interfacial spin-dependent electron scattering, while the broken line includes both interfacial and bulk spin-dependent scattering. In the notation of Ref. 5(a), $p_b=0$, $p_s=0.52$, and $\lambda_s=4.8a_0$ for the solid line and $p_b=0.17$, $p_s=0.50$, and $\lambda_s=4.6a_0$ for the broken line. The inset shows the Porod radii vs anneal temperature data.

data for the 450 °C annealed film are presented in Fig. 3. While the weak scattering at large q results in appreciable counting statistical noise, the data are well described by a straight line with zero slope in the limit of large q. This implies the Co-Cu interface is atomically abrupt ($\sigma \lesssim 2.0$ Å). Similar results are obtained for the films annealed at 350 and 550 °C. Owing to the limited range of the data, it is unclear if a reliable asymptotic slope can be extracted for the unannealed and 250 °C annealed samples.[7] However, assuming the slopes extracted are reliable, we find $\sigma \lesssim 3.5$ Å for these two films. These results indicate that the slight increase in Co-Cu solubility with temperature[17] does not broaden the interfaces of the films annealed at higher temperature.

Returning to the connection between cluster size and MR, note that the fundamental assumption underlying most models of giant MR is that the current is carried in two independent conduction channels corresponding to up-spin and down-spin electrons. The magnetic-field dependence of the resistivity is attributed to spin-dependent scattering occurring within the ferromagnetic clusters and/or at the magnetic-nonmagnetic interfaces.[5] If interfacial spin-dependent scattering is the dominant mechanism responsible for giant MR, then the MR should scale approximately as the cluster surface to volume ratio. Alternatively, if spin-dependent volume scattering dominates, then the MR should depend only weakly on cluster size. Examination of Fig. 4 reveals that the MR scales approximately as the inverse cluster size. This indicates that interfacial spin-dependent scattering is predominant.

To quantify this observation, we compare our data with a phenomenological model. In such models the bulk and interfacial spin-dependent scattering is represented by spin-dependent mean-free paths for interfacial scattering $\lambda_s^{\pm}$, and for scattering in the interior of the magnetic clusters $\lambda_m^{\pm}$ with $\pm$ denoting the electron spin. We have used a representative model [Ref. 5(a)] to examine the MR dependence upon cluster size and spin-dependent mean-free path.[18] Using Eqs. (5) and (6) of Ref. 5(a), the best least-squares fit to the MR data is obtained with no bulk spin-dependent scattering ($\chi^2=1.9$). This fit, the solid line in Fig. 4, implies that the interfacial electron scattering is strongly spin dependent with $\lambda_s^-/\lambda_s^+ \approx 10$.[19] Introducing even a slight spin dependence to the bulk scattering degrades the quality of the fit and significantly increases the interfacial spin-dependent scattering. For example, refitting the data with $\lambda_m^-/\lambda_m^+=2.0$, quadruples χ^2 while increasing λ_s^-/λ_s^+ to 36 (broken line, Fig. 4). It should be noted that this result is not crucially dependent upon the largest Porod radii datum, as excluding this datum from the fit yields similar results.[7] Thus, this analysis provides quantitative confirmation that interfacial spin-dependent scattering is the predominant scattering mechanism underlying giant MR in granular alloys.

In summary, we have used grazing incidence, anomalous SAXS to examine the relationship between cluster size and giant MR in phase-separated alloy films. With thermal annealing, the Co cluster characteristic diameter in $Co_{16}Cu_{84}$ films increased from 21 to ~250 Å with an associated decrease in the saturation MR from ~35 to 1 %. Our results demonstrate that the MR varies approximately as the inverse cluster size. Comparison with phenomenological theory indicates that interfacial spin-dependent electron scattering is the predominant scattering mechanism influencing giant MR for cluster diameters up to at least 250 Å. Finally, the rms width of the Co-Cu interface is $\lesssim 3.5$ Å.

Thanks to T. P. Russel and B. Stephenson for useful suggestions and S. Brennan for help with the anomalous form-factor calculation software. NSLS is supported by DOE Contract No. DE-AC02-76CH00016. X20 is supported by MIT through NSF Grant No. DMR 8719217 and by IBM Corp.

[1]M. N. Baibich, J. M. Broto, A. Fert, F. Nguyen van Dau, F. Petroff, P. Etienne, G. Creuzet, A. Friederich, and J. Chazeles, Phys. Rev. Lett. **61**, 2472 (1988).

[2]S. S. P. Parkin, N. More, and K. P. Roche, Phys. Rev. Lett. **64**, 2304 (1990).

[3]A. E. Berkowitz, J. R. Mitchell, M. J. Carey, A. P. Young, S. Zhang, F. E. Spada, F. T. Parker, A. Hutten, and G. Thomas, Phys. Rev. Lett. **68**, 3745 (1992).

[4]J. Q. Xiao, J. S. Jiang, and C. L. Chien, Phys. Rev. Lett. **68**, 3749 (1992); P. Xiong, G. Xiao, J. Q. Wang, J. Q. Xiao, J. S. Jiang, and C. L. Chien, *ibid.* **69**, 3220 (1992).

[5]S. Zhang, Appl. Phys. Lett. **61**, 1855 (1992); (b) S. Zhang and P. M. Levy, J. Appl. Phys. **73**, 5315 (1993).

[6]S. S. P. Parkin, R. F. C. Farrow, T. A. Rabedeau, R. F. Marks, G. R. Harp, Q. Lam, C. Chappert, M. Toney, R. Savoy, and R. Geiss, Europhys. Lett. **22**, 455 (1993).

[7]T. A. Rabedeau, M. F. Toney, R. F. Marks, S. S. P. Parkin, R. F. C. Farrow, and G. R. Harp (unpublished).

[8]D. H. Templeton in *Handbook on Synchrotron Radiation,* edited by G. Brown and D. E. Moncton (Elsevier Science, Amsterdam, 1991), Vol. 3, p. 201.

[9]T. P. Russell in *Handbook on Synchrotron Radiation,* edited by G. Brown and D. E. Moncton (Elsevier Science, Amsterdam, 1991), Vol. 3, p. 379; G. Porod in *Small Angle X-ray Scattering,* edited by O. Glatter and O. Kratky (Academic, London, 1982), p. 17.

[10]J. R. Levine, J. B. Cohen, and Y. W. Chung, Surf. Sci. **248**, 215 (1991).

[11]S. K. Sinha, E. B. Sirota, S. Garoff, and H. B. Stanley, Phys. Rev. B **38**, 2297 (1988).

[12]Since the films terminate in pure Cu layers, the surface diffuse scattering is independent of photon energy except for a scale factor. Diffuse scattering associated with roughness at the alloy-Cu cap interface is negligible owing to low scattering contrast (i.e., 0.4% of the cap-vapor contrast at 7692 eV).

[13]D. T. Cromer and D. Liberman, J. Chem. Phys. **53**, 1891 (1970), Acta Crystallogr. Sect. A **37**, 267 (1981); S. Brennan and P. L. Cowan, Rev. Sci. Instrum. **63**, 850 (1992).

[14]The background scale factor was extracted from the ratio of the 7692 eV (foreground) data to the 8710 eV (background) data at low angles, where the scattering is dominated by surface diffuse scattering.

[15]The Porod radius calculation requires evaluation of the integral $\int_0^\infty dq\, q^2 I(q)$ while the data are restricted to $q_1 \le q \le q_2$. To evaluate this integral we employed the standard approximations (Ref. 9): (i) for $q < q_1$ we used the linear approximation $q^2 I(q) \approx q q_1 I(q_1)$; (ii) for $q > q_2$ we utilized the Porod asymptotic law $q^2 I(q) = K \exp(-\sigma^2 q^2)/q^2$ with K a constant.

[16]E. F. Fullerton, D. M. Kelly, J. Guimpel, I. K. Schuller, and Y. Bruynseraede, Phys. Rev. Lett. **68**, 859 (1992).

[17]W. G. Moffatt, *The Handbook of Binary Phase Diagrams,* Vol. II (Genium, New York, 1984).

[18]The theory includes an implicit dependence on the cluster separation through the ferromagnetic concentration and the mean-free path in the nonmagnetic metal, λ_{nm}. The theory requires no assumptions regarding the relative size of λ_{nm} and the cluster size-separation. The model employs the simplifying assumption of a delta-function distribution of Co cluster sizes. The conclusions of our analysis are unchanged when the fits are repeated using a MR model [Ref. 5(b)] which includes a distribution of cluster sizes centered on the measured characteristic cluster sizes.

[19]In the notation of Ref. 5(a) $\lambda_m = 330$ Å and $\lambda_{nm} = 90$ Å at 4.2 K, S. S. P. Parkin (unpublished).